Reactive Intermediates in Peptide Synthesis: First Crystal Structures and *ab Initio* Calculations of 2-Alkoxy-5(4*H*)-oxazolones from Urethane-Protected Amino Acids

Marco Crisma,*[1a] Giovanni Valle,[1a] Fernando Formaggio,[1a] Claudio Toniolo,[1a] and Alessandro Bagno[1b]

Contribution from the Biopolymer Research Center, CNR, Department of Organic Chemistry, University of Padova, 35131 Padova, Italy, and the Organic Reaction Mechanism Research Center, CNR, Department of Organic Chemistry, University of Padova, via Marzolo 1, 35131 Padova, Italy

Received November 1, 1996[⊗]

Abstract: The structures of the 2-alkoxy-5(4*H*)-oxazolones derived from 2,2,6,6-tetramethyl-4-[(benzyloxycarbonyl)-amino]-1-oxypiperidine-4-carboxylic acid and 2,2,6,6-tetramethyl-4-[(9′-fluorenylmethoxycarbonyl)amino]-1-oxy-piperidine-4-carboxylic acid have been solved by single-crystal X-ray diffraction. The overall geometry of their oxazolone ring compares well with that of 2-alkyl-5(4*H*)-oxazolones. However, the bond distance from C_2 to the exocyclic O(2) atom is shorter than expected for a (sp^2)C−O single bond, thus suggesting a significant involvement of a O(2) lone pair in the electron delocalization of the C═N π-system. These two structures represent the first examples of 2-*alkoxy*-5(4*H*)-oxazolones in the crystal state. *Ab initio* molecular orbital calculations have been performed on (4*S*)-2-methoxy-4-methyl-5(4*H*)-oxazolone and (4*S*)-2,4-dimethyl-5(4*H*)-oxazolone [as simple models for 2-alkoxy- and 2-alkyl-5(4*H*)-oxazolones, respectively, derived from the chiral protein amino acid L-Ala] both in the neutral and deprotonated state. The calculated geometries of the 2-alkoxy- and 2-alkyl-5(4*H*)-oxazolone systems at the MP2/6-31+G(d,p) level agree well with those experimentally determined in the crystal state. The calculated energetics of deprotonation show only modest differences between the two systems. Conversely, a theoretical investigation of the reaction of model oxazolones with ammonia as a nucleophile indicates that for 2-alkoxy-5(4*H*)-oxazolones the activation energy of the rate-determining step is significantly lower and the overall stabilization energy is larger than for 2-alkyl-5(4*H*)-oxazolones. The implications of these results with respect to coupling and racemization of urethane-protected amino acids in peptide synthesis are outlined.

Introduction

2-Alkoxy-5(4*H*)-oxazolones (**I**, Chart 1) may originate from N^{α}-urethane-protected amino acids under a variety of activating conditions used for peptide bond formation. This phenomenon, first noticed by Jones and Witty,[2,3] has been extensively investigated by Benoiton and co-workers.[4] The extent of formation of 2-alkoxy-5(4*H*)-oxazolones depends upon the activation method, the nature of the amino acid side chain, and the type of urethane protecting group. Oxazolones (azlactones) of this type are in general rather unstable and difficult to isolate in a pure form. With few exceptions,[3,5,6] they have been obtained as oily products. Therefore, evidence for their occurrence has been obtained so far almost exclusively by spectroscopic techniques. Unexpectedly, 2-alkoxy-5(4*H*)-oxazolones from the Z and Fmoc derivatives of Toac (a spin-labeled, conformationally constrained, C^{α}-tetrasubstituted amino acid)[7] (**Ia** and **Ib**, respectively) turned out to be of high crystallinity and sufficient stability to be amenable to X-ray diffraction analysis.

Chart 1

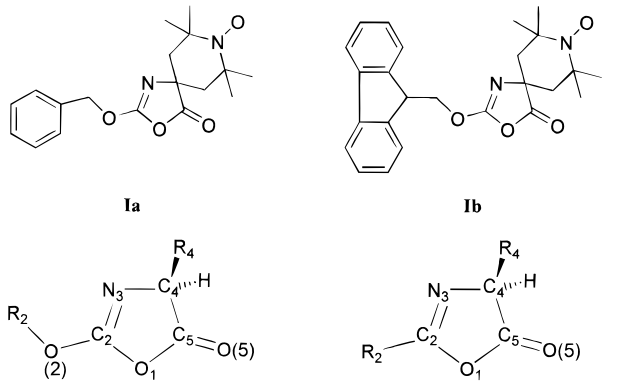

* Address for correspondence: Dr. Marco Crisma, Biopolymer Research Center, CNR, Department of Organic Chemistry, University of Padova, Via Marzolo 1, I-35131 Padova, Italy. E-mail: biop02@pdchor.chor.unipd.it.

⊗ Abstract published in *Advance ACS Abstracts,* March 15, 1997.

(1) (a) Biopolymer Research Center. (b) Organic Reaction Mechanism Center.

(2) Jones, J. H.; Witty, M. J. *J. Chem. Soc., Chem. Commun.* **1977**, 281−282.

(3) Jones, J. H.; Witty, M. J. *J. Chem. Soc., Perkin Trans. 1* **1979**, 3203−3206.

(4) Benoiton, N. L. *Biopolymers* **1996**, *40*, 245−254, and references therein.

(5) Benoiton, N. L; Chen, F. M. F. *Int. J. Pept. Protein Res.* **1994**, *42*, 455−458.

(6) Carpino, L. A.; Chao, H. G.; Beyermann, M.; Bienert, M. *J. Org. Chem.* **1991**, *56*, 2635−2642.

(7) Abbreviations: Toac, 2,2,6,6-tetramethyl-4-amino-1-oxypiperidine-4-carboxylic acid: Z, benzyloxycarbonyl; Fmoc, 9-fluorenylmethoxycarbonyl; Moc, methoxycarbonyl; Ac, acetyl.

S0002-7863(96)03786-9 CCC: $14.00

In this paper we report the crystal structures of the 2-alkoxy-5(4*H*)-oxazolones from Z-Toac-OH and Fmoc-Toac-OH, which allowed us to characterize for the first time the 2-alkoxy-5(4*H*)-oxazolone system at atomic resolution and to compare its geometry with that observed in the published crystal structures of 2-alkyl-5(4*H*)-oxazolones.[8−14]

Beginning with the pioneering work of Goodman,[15−17] ample evidence in the literature indicates that 2-alkyl-5(4*H*)-oxazolones (**II**) derived from N^{α}-acylated chiral (C^{α}-trisubstituted) amino acids or peptides give extensive racemization in peptide synthesis.[18] On the other hand, even if N^{α}-urethane-protected amino acids may give rise to some extent to the formation of 2-alkoxy-5(4*H*)-oxazolones upon activation, in general they can be safely employed in peptide synthesis without significant racemization.[18] In some cases experimental evidence has been provided that 2-alkoxy-5(4*H*)-oxazolones undergo aminolysis much faster and racemize more slowly than 2-alkyl-5(4*H*)-oxazolones.[3] Subsequently, however, the assumption that 2-alkoxy-5(4*H*)-oxazolones are inherently more chirally stable than their 2-alkyl counterparts has been questioned, since it has been shown that racemization (or epimerization) may be detected when peptide coupling is carried out with the former in the presence of a tertiary amine.[19] In addition, an example of a 2-alkoxy-5(4*H*)-oxazolone which autoracemizes upon storage has been recently reported.[20]

In this connection, we thought interesting to undertake *ab initio* molecular orbital calculations on simple model oxazolones, with the aim of gaining further insight on whether there are significant differences between 2-alkoxy- and 2-alkyl-5(4*H*)-oxazolones in terms of acidity and ease of being attacked by nucleophiles.

The evaluation of intrinsic acidities has been carried out on (4*S*)-2-methoxy-4-methyl-5(4*H*)-oxazolone (**Ic**) and (4*S*)-2,4-dimethyl-5(4*H*)-oxazolone (**IIc**) (*i.e.*, the oxazolones derived from Moc-L-Ala-OH and Ac-L-Ala-OH, respectively), both in the neutral and deprotonated states. As a model of the oxazolone-mediated peptide bond formation, a theoretical investigation of the addition mechanism of ammonia to oxazolones has been preliminarily performed on the least computationally demanding 2-hydroxy-5(4*H*)-oxazolone (**Id**) and 5(4*H*)-oxazolone (**IId**). The most favorable reaction path resulting from such screening has been further refined by theoretically investigating the addition of ammonia to 2-methoxy-5(4*H*)-oxazolone (**Ie**) and 2-methyl-5(4*H*)-oxazolone (**IIe**). A study on the mechanism of addition of ammonia or water to 2-methyl-5(4*H*)-oxazolone (**IIe**), carried out at a semiempirical level, was previously reported by Ciarkowski *et al*.[21]

Materials and Methods

Synthesis. The 2-alkoxy-5(4*H*)-oxazolones (**Ia**) and (**Ib**) were prepared from Z-Toac-OH[22] and Fmoc-Toac-OH,[23] respectively, by treatment with 1 equiv of *N*-ethyl-*N*′-[3-(dimethylamino)propyl]carbodiimide hydrochloride[19] at 0 °C for 2 h in anhydrous acetonitrile. The solvent was removed under reduced pressure. The resulting mixture was taken up in ethyl acetate, and the organic layer was washed with H_2O, 10% aqueous $KHSO_4$, H_2O, 5% aqueous $NaHCO_3$, and H_2O; dried over Na_2SO_4; and evaporated to dryness. The 2-alkoxy-5(4*H*)-oxazolones were recrystallized as indicated in ref 24 where analytical data have also been reported.

X-ray Diffraction. Single crystals of **Ia** and **Ib** were grown from ethyl acetate and chloroform−petroleum ether solutions, respectively. Diffraction data for both structures were collected on a Philips PW 1100 diffractometer, using Mo K_α radiation ($\lambda = 0.71073$ Å) in the θ - 2θ scan mode. Both structures were solved by direct methods with the SHELXS 86 program[25] and refined by full-matrix-blocked least-squares with all non-hydrogen atoms anisotropic using SHELX 76.[26] Most of the hydrogen atoms of both structures were located on a difference Fourier map, and the remaining ones were calculated. Hydrogen atoms of both **Ia** and **Ib** were refined in the riding mode with a fixed isotropic thermal parameter.

Crystal Data for the 5(4*H*)-Oxazolone from Z-Toac-OH (Ia): $C_{18}H_{23}N_2O_4$; $M = 331.4$; monoclinic; $a = 11.868(2)$, $b = 12.290(2)$, $c = 12.886(2)$ Å; $\beta = 103.0(2)°$; space group $P2_1/n$ (no. 14); $V = 1829(2)$ Å^3; $Z = 4$; $D_{calc} = 1.20$ g cm^{-3}; 2623 independent reflections collected up to $2\theta = 46.5°$; 1838 reflections with $F \geq 4\sigma(F)$ considered observed, refinement on F, weighting scheme $w = 1/[\sigma^2(F) + 0.0019F^2]$; $R = 0.056$; $R_w = 0.064$; goodness of fit = 0.668.

Crystal Data for the 5(4*H*)-Oxazolone from Fmoc-Toac-OH (Ib): $C_{25}H_{27}N_2O_4$; $M = 419.5$; monoclinic; $a = 8.266(1)$, $b = 18.629(2)$, $c = 14.216(2)$ Å; $\beta = 98.6(1)°$; space group $P2_1/n$ (no. 14); $V = 2164.5(7)$ Å^3; $Z = 4$; $D_{calc} = 1.29$ g cm^{-3}; 2266 independent reflections collected up to $2\theta = 41.6°$; 1097 reflections with $F \geq 4\sigma(F)$ considered observed; refinement on F, weighting scheme $w = 1/[\sigma^2(F) + 0.0037F^2]$; $R = 0.051$; $R_w = 0.053$; goodness of fit = 0.996.

Complete lists of bond distances, bond angles and the final positional parameters for all non-hydrogen atoms along with their thermal factors for both structures have been deposited and are available from the Cambridge Crystallographic Data Centre (Cambridge, UK).

Theoretical Calculations. The calculation of the intrinsic acidities of (4*S*)-2-methoxy-4-methyl-5(4*H*)-oxazolone (**Ic**), (4*S*)-2,4-dimethyl-5(4*H*)-oxazolone (**IIc**), and their corresponding deprotonated forms was carried out by *ab initio* methods. A reliable calculation of the proton affinity of anions requires the inclusion of diffuse functions in the basis set, correcting the energy for electron correlation, and the evaluation of the zero-point vibrational energy (ZPE) to account for the motion of the molecule even at 0 K.[27] The basis set chosen is the double split-valence 6-31G set, augmented with d and diffuse functions on non-hydrogen atoms [6-31+G(d)].[27] Thus, the four structures have been optimized at the HF/6-31+G(d) level of theory, and ZPEs were

(8) Flippen-Anderson, J. L.; George, C.; Valle, G.; Valente, E.; Bianco, A.; Formaggio, F.; Crisma, M.; Toniolo, C. *Int. J. Pept. Protein Res.* **1996**, *47*, 231−238.
(9) Nair, C. M. K.; Vijayan, M. *Acta Crystallogr.* **1980**, *B36*, 1498−1500.
(10) Toniolo, C.; Bonora, G. M.; Crisma, M.; Benedetti, E.; Bavoso, A.; Di Blasio, B.; Pavone, V.; Pedone, C. *Int. J. Pept. Protein Res.* **1983**, *22*, 603−610.
(11) Toniolo, C.; Valle, G.; Formaggio, F.; Crisma, M.; Boesten, W. H. J.; Polinelli, S.; Schoemaker, H. E.; Kamphuis, J. *J. Chem. Soc., Perkin Trans. 1* **1991**, 3386−3388.
(12) Valle,G.; Crisma, M.; Pantano, M.; Formaggio, F.; Toniolo, C.; Kamphuis, J. *Zeit. Kristallogr.* **1993**, *208*, 259−262.
(13) Crisma, M.; Formaggio, F.; Pantano, M.; Valle, G.; Bonora, G. M.; Toniolo, C.; Schoemaker, H. E.; Kamphuis, J. *J. Chem. Soc., Perkin Trans. 2* **1994**, 1735−1742.
(14) Crisma, M.; Valle, G.; Moretto, V.; Formaggio, F.; Toniolo, C. *Pept. Res.* **1995**, *8*, 187−190.
(15) Goodman, M.; Stueben, K. C. *J. Org. Chem.* **1962**, *27*, 3409−3416.
(16) Goodman, M.; McGahren, W. H. J. *J. Am. Chem. Soc.* **1965**, *87*, 3028−3029.
(17) Goodman, M.; McGahren, W. H. J. *Tetrahedron* **1967**, *23*, 2031−2050.
(18) Kemp, D. S. In *The Peptides. Analysis, Synthesis, Biology;* Gross, E., Meienhofer, J., Eds.; Academic Press: New York, 1979; Vol. 1, pp. 315−383.
(19) Benoiton, N. L.; Chen, F. M. F. *Can. J. Chem.* **1981**, *59*, 384−389.
(20) Benoiton, N. L.; Lee, Y. C.; Steinauer, R. *Pept. Res.* **1995**, *8*, 108−112.
(21) Ciarkowski, J.; Chen, F. M. F.; Benoiton, N. L. *J. Comput.-Aided Mol. Design* **1991**, *5*, 585−597.
(22) Dulog, L.; Wang, W. *Liebigs Ann. Chem.* **1992**, 301−303.
(23) Marchetto, R.; Schreier, S.; Nakaie, C. R. *J. Am. Chem. Soc.* **1993**, *115*, 11042−11043.
(24) Toniolo, C.; Valente, E.; Formaggio, F.; Crisma, M.; Pilloni, G.; Corvaja, C.; Toffoletti, A.; Martinez, G. V.; Hanson, M. P.; Millhauser, G. L.; George, C.; Flippen-Anderson, J. L. *J. Pept. Sci.* **1995**, *1*, 45−57.
(25) Sheldrick, G. M. In *Crystallographic Computing 3*; Sheldrick, G. M., Kruger, C., Goddard, R., Eds.; Oxford University Press: Oxford, UK, 1985; pp 175−189.
(26) Sheldrick, G. M. *Program for Crystal Structure Determination*; University of Cambridge: Cambridge, UK, 1976.
(27) Hehre, W. J.; Radom, L.; Schleyer. P. v. R.; Pople, J. A. *Ab Initio Molecular Orbital Theory*; Wiley-Interscience: New York, 1986.

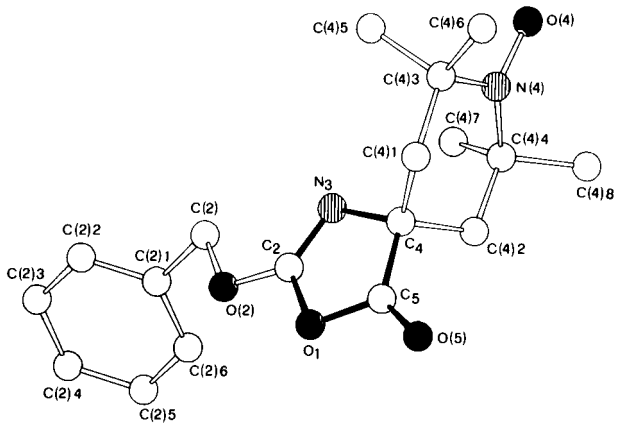

Figure 1. X-ray structure of the 2-alkoxy-5(4*H*)-oxazolone derived from Z-Toac-OH (**Ia**). Nitrogen and oxygen atoms are represented as dashed and filled circles, respectively. The oxazolone ring is highlighted.

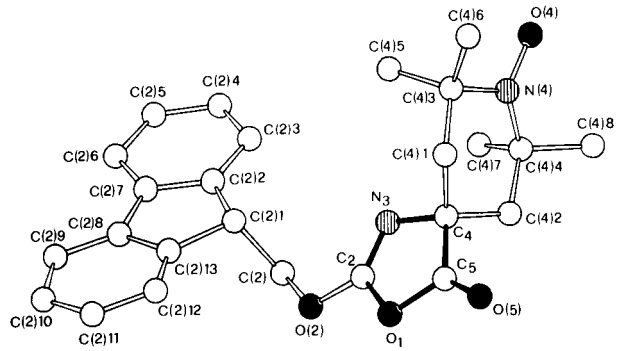

Figure 2. X-ray structure of the 2-alkoxy-5(4*H*)-oxazolone derived from Fmoc-Toac-OH (**Ib**). Nitrogen and oxygen atoms are represented as dashed and filled circles, respectively. The oxazolone ring is highlighted.

calculated at that geometry. The correlation energy correction was estimated via second-order Møller−Plesset perturbation theory (MP2) in the frozen-core approximation, at the HF/6-31+G(d) geometry with a more extended basis set; thus, the overall level of calculation is denoted as MP2(FC)/6-31+G(d,p)//HF/6-31+G(d).[27] Zero-point energies were scaled by 0.89 before inclusion in the total energy.[27] Atomic charges were calculated from fits to electrostatic potential maps, using a grid of 1 Å/atomic unit.

The above level of calculation is adequate for describing the ionization process in the gas phase. However, in order to estimate also the solvent influence, we carried out calculations employing the self-consistent reaction field method (SCRF).[28−30] This method represents the solvent as a continuum with a given permittivity, and assumes the solute molecule to be spherical with a radius a_0. The latter parameter was calculated by Monte Carlo integration at the HF/6-31+G(d) level, and the typical solvent dichloromethane ($\epsilon = 8.9$) was chosen for the calculations.

The stationary points on the potential energy surface (PES) for the addition of NH_3 to model oxazolones have been characterized by geometry optimization and vibrational analysis at the HF/6-31G(d) level. The initial geometry of transition states was estimated by linear synchronous transit between the previously optimized structures of reactants and products. For transition states, we verified that there was only one imaginary frequency, corresponding to the vibration connecting reactants to products.

All calculations were carried out with the *Spartan*[31] and *Gaussian 92*[32] programs, running on an IBM RS/6000 workstation.

Results

X-ray Structures. The structures of the 5-(4*H*)-oxazolones from Z-Toac-OH (**Ia**) and from Fmoc-Toac-OH (**Ib**), solved by X-ray diffraction, are illustrated in Figures 1 and 2, respectively. Bond distances and angles (deposited) about the Toac cyclic side chain observed in these structures are in general agreement with those reported for other Toac derivatives and peptides.[8,24] In particular, the N−O bond distance of the nitroxide group is 1.293(3) and 1.276(7) Å in **Ia** and **Ib**, respectively, significantly shorter than the typical length for a (sp^2)N−O single bond (1.39−1.40 Å).[33,34]

In both structures the piperidine ring of the Toac side chain is close to the chair conformation, with the following puckering parameters: $Q_T = 0.487(5)$ Å, $\phi_2 = 177(1)°$, $\theta_2 = 27.8(6)°$ for **Ia**, and $Q_T = 0.499(6)$ Å, $\phi_2 = 179(2)°$, $\theta_2 = 14.0(6)°$ for **Ib**.[35] The piperidine ring is nearly perpendicular to the oxazolone ring, the angles between normals to the corresponding average planes being 92° and 90° in **Ia** and **Ib**, respectively. In the structure of **Ia** the angle between normals to the average planes of the oxazolone and phenyl rings is 66°, while the angle between normals to the average planes of the oxazolone and fluorenyl rings found in the structure of **Ib** is 27°.

In both structures the oxazolone ring is nearly planar. The displacement of the ring atoms from the ring mean plane vary from −0.016 to 0.017 Å and from −0.016 to 0.009 Å in **Ia** and **Ib**, respectively. In both structures the exocyclic O(5) atom is nearly coplanar to the oxazolone ring, with a displacement of −0.004(3) Å and 0.014(4) Å in **Ia** and **Ib**, respectively, while the O(2) atom deviates from the plane by 0.115(3) Å in **Ia**, and −0.060(4) Å in **Ib**.

Bond distances and angles about the 2-alkoxy-5(4*H*)-oxazolone moiety, averaged from the two structures described in this paper, are reported in Table 1A and compared with bond distances and angles averaged from published X-ray structures of 2-alkyl-5(4*H*)-oxazolones.[8−14]

Most of the bond distances and angles are nearly identical in the two systems. Particularly noteworthing is the exact matching of the $C_2{=}N_3$ and $C_5{=}O(5)$ bond distances. Small (though significant) differences between 2-alkoxy- and 2-alkyl-substituted 5(4*H*)-oxazolones, however, are observed for (i) the O_1-C_2 bond distance, which is 0.02 Å shorter in the former, thus suggesting a slightly more effective intra-ring electron delocalization in the 2-alkoxy-5(4*H*)-oxazolones, and (ii) for the bond angles about the O_1, C_2, and N_3 atoms. Bond angles at O_1 and N_3 are 2° larger in the 2-alkyl-5(4*H*)-oxazolones, whereas the endocyclic $O_1-C_2-N_3$ bond angle is 3° larger in the 2-alkoxy-5(4*H*)-oxazolones. In addition, in the 2-alkoxy-5(4*H*)-oxazolones the exocyclic $O(2)-C_2-N_3$ bond angle is 2° larger and the exocyclic $O(2)-C_2-O_1$ bond angle is 5° narrower than the corresponding $C(2)-C_2-N_3$ and $C(2)-C_2-O_1$ bond angles observed in the 2-alkyl-5(4*H*)-oxazolone system.

The most striking geometrical feature of the 2-alkoxy-5(4*H*)-oxazolone system, however, is the length of the exocyclic C_2-

(28) Wong, M. W.; Frisch, M. J.; Wiberg, K. B. *J. Am. Chem. Soc.* **1991**, *113*, 4776−4782.
(29) Wong, M. W.; Wiberg, K. B.; Frisch, M. J. *J. Am. Chem. Soc.* **1992**, *114*, 523−529.
(30) Wong, M. W.; Wiberg, K. B.; Frisch, M. J. *J. Am. Chem. Soc.* **1992**, *114*, 1645−1652.
(31) *Spartan v. 3*, Wavefunction, Irvine, CA, 1993.
(32) Frisch, M. J.; Trucks, G. W.; Schlegel, H. B.; Gill, P. M. W.; Johnson, B. G.; Wong, M. W.; Foresman, J. B.; Robb, M. A.; Head-Gordon, M.; Reprogle, E. S.; Gomperts, R.; Andres, J. L.; Raghavachari, K.; Binkley, J. S.; Gonzales, C.; Martin, R. L.; Fox, D. J.; Defrees, D. J.; Baker, J.; Stewart, J. J. P.; Pople, J. A. *Gaussian 92/DFT*, revision F.2, Gaussian Inc.: Pittsburgh, PA, 1993.
(33) Allen, F. H.; Kennard, O.; Watson, D. G.; Brammer, L.; Orpen, A. G.; Taylor, R. *J. Chem. Soc., Perkin Trans. 2* **1987**, S1−S19.
(34) Lajzerowicz-Bonneteau, J. In *Spin Labelling. Theory and Applications*; Berliner, L. J., Ed.; Academic Press: New York, 1976; pp 239−249.
(35) Cremer, D.; Pople, J. A. *J. Am. Chem. Soc.* **1975**, *97*, 1354−1358.

Table 1. (**A**) Selected Bond Distances (Å) and Angles (deg) for the 2-Alkoxy- and 2-Alkyl-5(4*H*)-oxazolone Moieties As Averaged from the X-ray Structures and (**B**) Corresponding Bond Distances (Å) and Angles (deg) As Obtained by *ab Initio* Calculations on 2-Methoxy-4-Methyl-5(4*H*)-oxazolone (**Ic**) and 2,4-Dimethyl-5(4*H*)-oxazolone (**IIc**), and Their Corresponding Deprotonated Forms (**Ic**$^-$ and **IIc**$^-$)

	(A) from X-ray structures[a]		(B) *ab initio* HF/6-31+G(d) geometry optimization			
	2-alkoxyoxazolones (**I**)[b]	2-alkyloxazolones (**II**)[c]	2-alkoxyoxazolone (**Ic**)	2-alkyloxazolone (**IIc**)	2-alkoxy anion (**Ic**$^-$)	2-alkyl anion (**IIc**$^-$)
O_1-C_2	1.37	1.39	1.349	1.369	1.313	1.341
C_2-N_3	1.26	1.26	1.253	1.250	1.258	1.266
N_3-C_4	1.47	1.47	1.453	1.453	1.424	1.402
C_4-C_5	1.52	1.53	1.523	1.520	1.366	1.376
O_1-C_5	1.38	1.38	1.364	1.356	1.442	1.408
$C_2-O(2)$	1.32	–	1.298	–	1.340	–
$C_2-C(2)$	–	1.49	–	1.487	–	1.491
$C_5-O(5)$	1.19	1.19	1.174	1.176	1.231	1.234
$C_2-O_1-C_5$	104	106	106.2	107.0	105.3	106.6
$O_1-C_2-N_3$	120	117	118.4	116.6	117.4	114.3
$C_2-N_3-C_4$	105	107	106.1	107.1	103.5	105.4
$N_3-C_4-C_5$	104	104	103.4	103.3	110.3	109.7
$O_1-C_5-C_4$	107	107	106.0	105.9	103.5	104.0
$O_1-C_2-O(2)$	111	–	112.5	–	114.7	–
$O_1-C_2-C(2)$	–	116	–	115.0	–	117.5
$N_3-C_2-O(2)$	129	–	129.1	–	127.9	–
$N_3-C_2-C(2)$	–	127	–	128.4	–	128.1
$O_1-C_5-O(5)$	122	122	122.9	123.3	118.0	119.1
$C_4-C_5-O(5)$	131	131	131.2	130.8	138.5	137.0
$O_1-C_2-O(2)-CH_3$			180.0		179.9	

[a] Estimated standard deviations: ≤ 0.01 Å for bond distances; ≤ 1° for bond angles. [b] This work. [c] References 8−14. The structures of 2-aryl-5(4*H*)-oxazolones and 4-alkylidene-5(4*H*)-oxazolones have not been considered.

Table 2. *Ab Initio* Energetics of Deprotonation of **Ic** and **IIc**

species	E[a]	ZPE (au)[b]	E_{tot} (au)[c]	PA of anion[d]	a_0[e]	E (CH_2Cl_2)[f]	ΔE (CH_2Cl_2)[g]
Ic	−473.856 873 2	0.134 348 6	−473.737 302 9	–	4.13	−472.475 206 9	–
Ic$^-$	−473.286 919 6	0.118 617 5	−473.181 350 0	348.9	4.17	−471.888 009 7	368.5
IIc	−398.829 382 7	0.127 139 0	−398.716 229 0	–	4.06	−397.619 919 8	–
IIc$^-$	−398.262 787 6	0.112 563 0	−398.162 606 5	347.4	4.10	−397.033 921 9	367.7

[a] In au, at MP2(FC)/6-31+G(d,p)//HF/6-31+G(d) level. [b] In au, at HF/6-31+G(d) level. [c] Including zero-point energies scaled by 0.89. [d] Energy difference (in kcal/mol) between neutral and anion at MP2 level, with ZPE correction. [e] Molecular radius in Å, at HF/6-31+G(d) level. [f] At SCRF/6-31+G(d)//HF/6-31+G(d) level, with the specified a_0 and a permittivity of 8.9 (CH_2Cl_2). [g] Energy difference between neutral and anion at SRCF level, without ZPE correction.

O(2) bond (1.32 Å), significantly shorter than expected for a (sp^2)C−O single bond (1.37−1.38 Å).[33] The average bond angle at the O(2) atom is 114°. In addition, the value of the $N_3-C_2-O(2)-C(2)$ torsion angle is −7.3(6) and −5.3(9)° in **Ia** and **Ib**, respectively. Such a planar arrangement of the N_3, C_2, O(2) and C(2), atoms allows the proper positioning of a lone pair of the O(2) atom for its effective interaction with the $C_2=N_3$ π-system.

Theoretical Calculation of the Structure and Acidity of Ic and IIc. Bond distances and angles of (4*S*)-2-methoxy-4-methyl-5(4*H*)-oxazolone (**Ic**), (4*S*)-2,4-dimethyl-5(4*H*)-oxazolone (**IIc**), and their corresponding deprotonated forms (**Ic**$^-$) and (**IIc**$^-$), as obtained by *ab initio* calculations, are reported in Table 1B. Apart for a general shortening of about 0.01−0.02 Å of the bond distances obtained *ab initio* for the 2-alkoxy- and 2-alkyl-5(4*H*)-oxazolone systems as compared with the corresponding ones averaged from the crystal structures (Table 1A), an excellent agreement is observed between calculated and experimental values. In particular, the calculations correctly reproduce the experimentally determined similarities and differences in terms of bond distances between the 2-alkoxy- and 2-alkyl-5(4*H*)-oxazolone systems. For instance, the O_1-C_2 bond distance is predicted to be 0.01 Å shorter than the O_1-C_5 bond distance in **Ic**, while this trend is reversed in **IIc**. Similarly, the values of the bond angles predicted by *ab initio* calculations are within 1−2° close to the corresponding ones averaged from the crystal structures (Table 1).

Interestingly, in the 2-alkoxy-5(4*H*)-oxazolone (**Ic**) structure calculated *ab initio* the $N_3-C_2-O(2)-C(2)$ torsion angle is 0.07°. Thus, the N_3-C_2 and $O(2)-C(2)$ bonds are eclipsed as observed in the crystal state, an indication that such an arrangement is not determined by crystal packing.

The results of the *ab initio* acidity calculations are summarized in Table 2. It can be seen that in the gas phase the proton affinities of the anions **Ic**$^-$ and **IIc**$^-$ differ by only 1.5 kcal/mol, **IIc** being slightly more acidic than **Ic**. In view of these small differences, we have decided to check whether a typical solvent for peptide coupling (dichloromethane) might have any influence on the relative acidities. Table 2 shows that inclusion of the solvent effect levels off relative acidities even more ($\Delta\Delta E$ = 0.8 kcal/mol). This result is not surprising, considering the weak solvation of delocalized carbanions, particularly in nonpolar solvents.

Theoretical Investigation of the Addition Mechanism. We have just demonstrated that the different chemical behavior of 2-alkyl- and 2-alkoxy-5(4*H*)-oxazolones cannot be ascribed to a different acid strength. Therefore, as a further step, we have theoretically investigated the reactivity of these important intermediates in peptide synthesis toward nucleophiles. The general reaction scheme in peptide coupling involves the nucleophilic attack of an amine to the carbonyl group of the oxazolone, followed by ring opening and tautomerization to the final product, as depicted in Scheme 1.

We have theoretically investigated the addition mechanism using NH_3 as the model nucleophile. A first screening of the

Table 3. Energies of Reacting Species in the Addition of NH_3 to Oxazolones **Id** and **IId**[a]

species	Id		IId		process
	E	Δ*E*	*E*	Δ*E*	
NH_3	−56.184 356				
oxazolone	−394.395 254		−319.521 399		
oxazolone + NH_3	−450.579 610	(0.0)	−375.705 760	(0.0)	
A	−450.587 324	−4.8	−375.713 011	−4.5	
B	−450.494 348	+58.3	−375.618 890	+59.1	**A** → **B**
C	−450.578 137	+5.6	−375.703 211	+6.1	**A** → **C**
D	−450.552 486	+16.1	−375.667 486	+22.4	**C** → **D**
E	−450.599 860	−13.6	−375.721 456	−11.4	**C** → **E**
F	−450.636 319	−22.9	−375.748 650	−17.1	**E** → **F**
G	−450.529 655	+36.2	−375.647 263	+41.2	**A** → **G**

[a] Energies in au, and Δ*E*'s in kcal/mol at the HF/6-31G(d) level, without vibrational energies.

Scheme 1

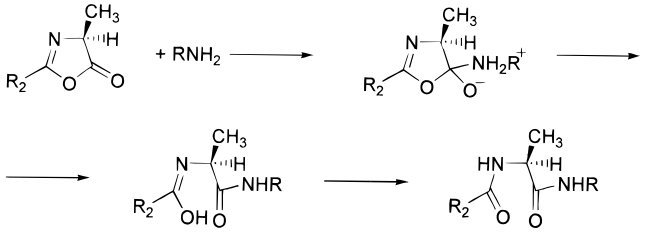

Scheme 2

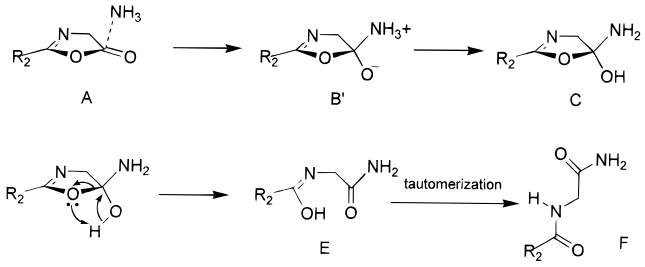

Scheme 3

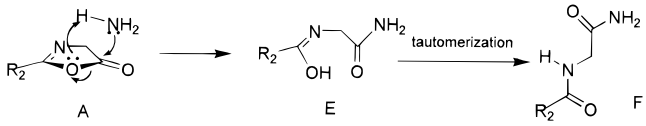

possible mechanisms has been run on simple model compounds **Id** and **IId**, analogues of **Ic** and **IIc**, respectively.

Two main pathways can be envisaged for this reaction, both involving an oxazolone−NH_3 complex, weakly bonded through the carbonyl carbon, as the initial structure **A** (Schemes 2 and 3). The first path, represented in Scheme 2, involves addition to the carbonyl group, yielding the usual tetrahedral adduct (**C**) through the zwitterionic species (**B′**). Intermediate **C** then undergoes ring opening, yielding the enol imine **E**, which eventually tautomerizes to the final amide product **F**.

The second pathway is a concerted addition−ring opening process leading directly to **E** and **F**, as in Scheme 3. All stationary points found are depicted below (Charts 2 and 3; species **A**, **E**, and **F** are common to both mechanisms). The energies of all species are reported in Table 3, and the structures of some stationary points (**A**, **B**, **D**, **G**) are depicted in Figure 3.

Stepwise Path. The initial formation of the oxazolone−NH_3 complex is slightly stabilizing, by *ca.* 5 kcal/mol. The zwitterionic species **B′** is not a stationary point on the PES. This observation is not unexpected, because any structure with a large charge separation like this is not favored in the gas phase. However, there is a minimum (**C**) in which proton transfer has

Chart 2. Stationary Points on the PES for the Stepwise Path

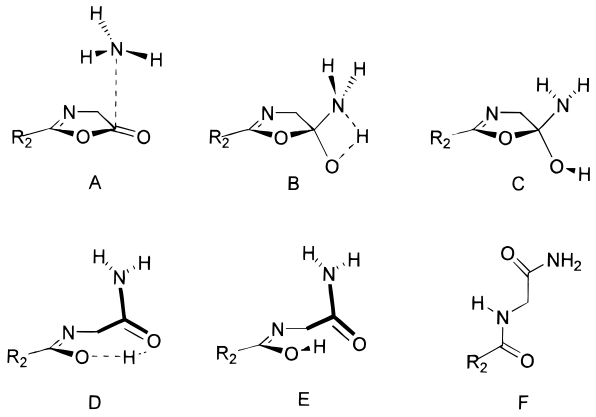

Chart 3. Stationary Point (Transition State) on the PES for the Concerted Path

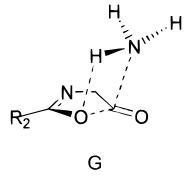

already occurred. The latter is less stable than **A** by about 6 kcal/mol; the transition state (**B**) connecting **A** and **C** is quite high in energy (E_a = 58−59 kcal/mol), which can be accounted for by noting the extensive rehybridization needed for the carbonyl carbon to reach an essentially tetrahedral geometry. Ring opening of **C** proceeds through the transition state **D** with an activation energy of 16−20 kcal/mol; at the transition state, the ring is essentially open (O_1−C_5 distance 2.440 Å) before the proton transfer to O_1 takes place appreciably, which indicates that ring opening is a driving force for the reaction. The overall process **C** → **E** is energetically favorable. **E** then tautomerizes to the final product **F** by a proton transfer which is probably intermolecular and fast; therefore, no transition state was searched for this step. Tautomerization to the amide is a major driving force for the process.

Concerted Path. The mechanism whereby NH_3 addition takes place concertedly with ring opening, leading to **E** through the transition state **G** has a lower activation energy (30−40 kcal/mol). The vibration connecting reactant (**A**) to product (**E**) in **G** is indeed an N−H proton transfer concerted with O_1−C_5 bond breaking. In fact, in the structure of **D** the carbonyl group retains its planar configuration (hence, with no need for extensive rehybridization as in the case of **B**). This transition state is reactant-like, because the N−H bond is very slightly lengthened, and the O_1−C_5 bond goes from 1.36 to 2.00 Å. Hence, the

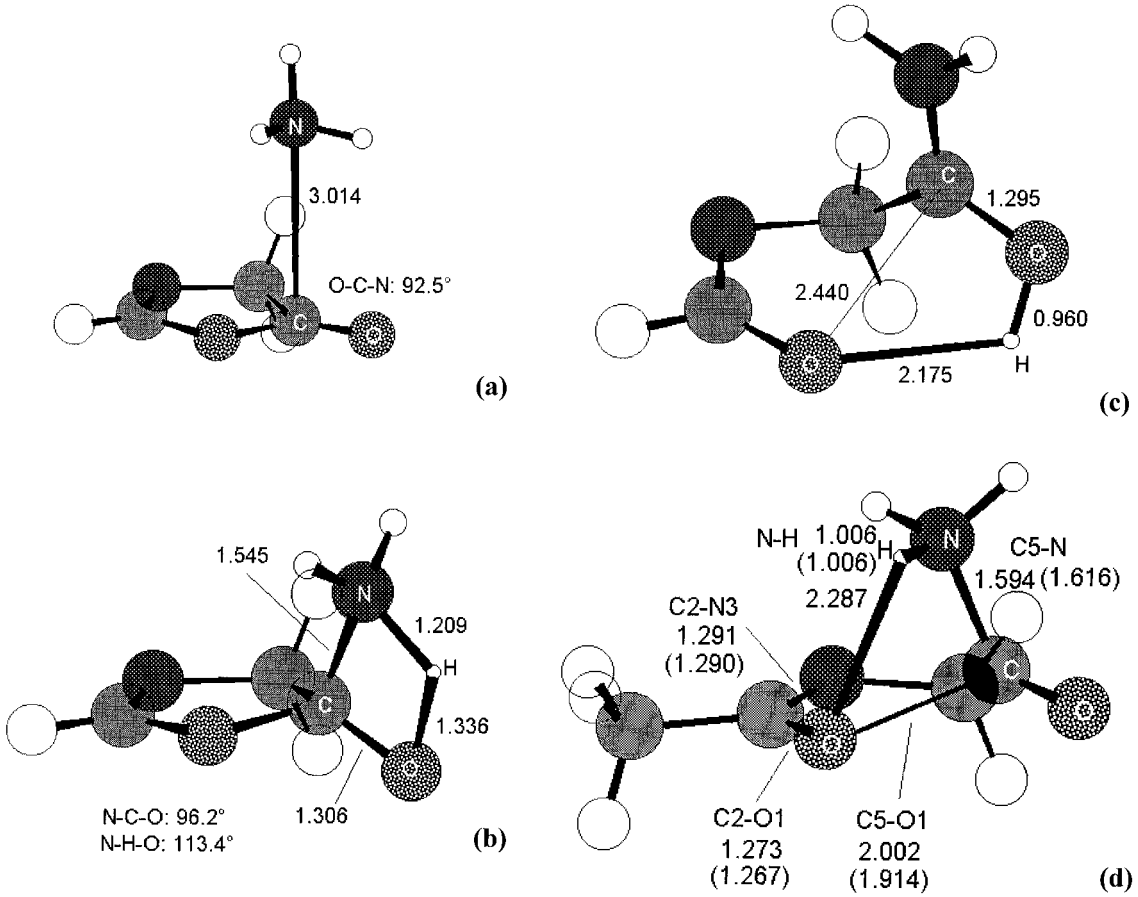

Figure 3. Structures of the main stationary points on the PES for the addition of NH_3 to model oxazolones [HF/6-31G(d) level]: (a) intermediate **A** (**IId**); (b) transition state **B** (**IId**); (c) transition state **D** (**IId**); (d) transition state **G** (**IIe**); data in parentheses refer to **Ie**. Distances in angstroms; angles in degrees. C, light grey; H, white; N, dark grey; O, dotted.

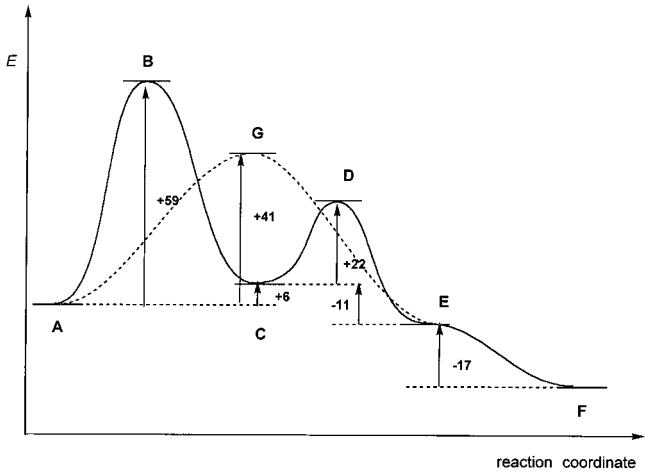

Figure 4. Energy profiles (kcal/mol) for the stepwise (solid line) and concerted (dashed line) addition of NH_3 to model oxazolone **IId**.

process is not synchronous, C−O bond breaking being more advanced than O−H bond formation. Unlike the reaction **A** → **C** of the stepwise path, the reaction **A** → **E** is energetically favorable (by 5−8 kcal/mol).

The two reaction profiles for **Id** and **IId** can now be compared. All data are collected in Table 3; for clarity, Figure 4 reports only the PES for **IId**.

It is apparent that the concerted pathway is more favored, because of its lower overall activation energy (Figure 4). It is also clear at this stage that **Id** (R_2 = OH) is more reactive than **IId** (R_2 = H) because of the lower activation energy of the **A** → **G** step and because of a larger stabilization following all reaction steps.

Thus, as a further step, the investigation was extended to models **Ie** and **IIe**, more closely related to peptide synthesis, comparing only the most favorable mechanism (concerted NH_3 addition). In this case, vibrational energies were also calculated. The results are collected in Table 4 and Figure 5.

Also in this case the calculations indicate a higher reactivity of the 2-alkoxy-5(4*H*)-oxazolone **Ie** relative to its 2-alkyl counterpart **IIe**. In particular, the former requires a lower activation energy in the **A** → **G** step (by 5.1 kcal/mol), and its reaction is accompanied by a larger overall stabilization energy (by 10 kcal/mol). The structure of the two transition states is only slightly different otherwise (Figure 3d). The lower activation energy for the alkoxy derivative **Ie** can be accounted for by recalling that the transition state **G** is reached when the proton transfer from NH_3 to O_1 has only negligibly progressed, but the O_1-C_5 bond (*ca.* 2 Å) is essentially broken. The calculated atomic charges on the hydrogen being transferred (*ca.* +0.3) and on O_1 (*ca.* −0.7) are consistent with a substantial degree of charge separation, so that the structure of **G** can be depicted as an open $R_2C(O^-)=NCH_2C(O)NH_3^+$ zwitterion. Other factors being equal, therefore, that species will be more stabilized by substituents capable of removing excess negative charge from the oxygen. Thus, the observed larger stabilization of **G**(**Ie**) relative to **G**(**IIe**) is consistent with the electron-withdrawing inductive effect of the methoxy group; actually, the CH_3 and CH_3O groups in **G** bear a partial charge of −0.13 and −0.28, respectively.

Table 4. Energies of Reacting Species in the Addition of NH_3 to Oxazolones **Ie** and **IIe**[a]

	Ie			**IIe**			
species	*E*	ZPE[b]	ΔE[c]	*E*	ZPE[b]	ΔE[c]	process
NH_3	−56.184 356	23.22					
oxazolone	−433.423 022	65.66		−358.570 829	61.68		
oxazolone + NH_3	−489.607 378	88.88	(0.0)	−414.755 185	84.90	(0.0)	
A	−489.614 657	90.17	−3.4	−414.761 894	86.12	−3.1	
E	−489.624 665	92.30	−4.4	−414.767 163	88.30	−1.1	**A** → **E**
F	−489.661 923	91.38	−24.2	−414.793 859	87.35	−17.7	**E** → **F**
G	−489.553 531	91.96	+39.9	−414.692 830	88.00	+45.0	**A** → **G**
			−28.8			−18.8	overall[d]

[a] Energies (au), ΔE's (kcal/mol), and zero-point vibrational energies calculated at the HF/6-31G(d) level. [b] Zero-point energies in kcal/mol, not scaled. [c] With ZPEs scaled by 0.89. [d] ΔE(**A** → **E**) + ΔE(**E** → **F**).

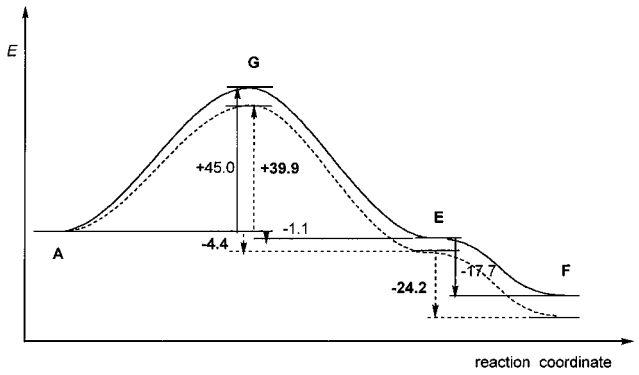

Figure 5. Energy profiles (kcal/mol) for the concerted addition of NH_3 to model oxazolones **Ie** (dashed line, boldface numbers) and **IIe** (solid line, plain numbers).

Discussion

The crystal structures of the oxazolones from Z-Toac-OH (**Ia**) and Fmoc-Toac-OH (**Ib**) have allowed for the first time the characterization at atomic resolution of 2-alkoxy-5(4*H*)-oxazolones from *N*-urethane-protected amino acids. These two structures suggest that in the 2-alkoxy-5(4*H*)-oxazolones a lone pair of the exocyclic O(2) atom is significantly involved in the electron delocalization of the C_2═N_3 π-system. The partial double-bond character of the C_2-O(2) bond may explain the easy decomposition of 2-*tert*-butoxy-5(4*H*)-oxazolones to give the corresponding (unprotected) *N*-carboxy anhydrides where such a bond is double.[19,36,37] On the other hand, the overall geometry of the oxazolone ring, as derived from the structures of these 2-alkoxy-5(4*H*)-oxazolones, compares well with that observed in the crystal structures of 2-alkyl-5(4*H*)-oxazolones.[8−14]

We have carried out *ab initio* molecular orbital calculations on (4*S*)-2-methoxy-4-methyl-5(4*H*)-oxazolone (**Ic**) and (4*S*)-2,4-dimethyl-5(4*H*)-oxazolone (**IIc**), respectively, as well as on their corresponding deprotonated forms $\mathbf{Ic}^-$ and $\mathbf{IIc}^-$. The calculated structures of the 2-alkoxy- and 2-alkyl-5(4*H*)-oxazolone systems, optimized at the Hartree−Fock 6-31+G(d) level of theory, show bond distances and angles in good agreement with those experimentally determined in the crystal state. On energetic grounds, by comparison of the proton affinities of anions $\mathbf{Ic}^-$ and $\mathbf{IIc}^-$, in the gas phase as well as including the solvation effect of dichloromethane, it appears that 2-alkyl-5(4*H*)-oxazolones (**II**) are only slightly more acidic than their 2-alkoxy counterparts (**I**).

Ciarkowski *et al.*[21] investigated the mechanism of addition of NH_3 and H_2O to the model oxazolone **IIe** at the semiempirical MNDO and AM1 levels, exploring the PES with regard to the possibility of either (a) direct conversion of the oxazolone−NH_3 complex **A** to the amide **F**, or (b) to the enol imine **E**, followed by tautomerization to **F** (Scheme 3). The conventional carbonyl addition (Scheme 2) was not considered. They found the activation energy for the direct process (**A** → **F**) to be quite high (50−60 kcal/mol); this is not surprising, because such a process would require an extensive atomic and electronic reorganization. Conversely, they found a lower barrier (27−41 kcal/mol) for the process **A** → **E**. However, the effect of the substituent at C_2 (CH_3 or OCH_3) on the reactivity toward NH_3 was not studied.

Our mechanistic investigation of NH_3 addition to oxazolones has shown that a major difference exists in the relative reactivity of **Ie** and **IIe** (and also of the simpler models **Id** and **IId**) toward nucleophiles. For both mechanistic pathways considered (Schemes 2 and 3), the derivatives containing OH or OCH_3 at C_2 are more reactive than the corresponding ones with H or CH_3, because the activation energy is lower, and the energetic gain is larger in the overall reaction. In fact, for the most likely reaction path (concerted NH_3 addition) the activation energy of the rate-determining step (**A** → **G**) of **Ie** is lower than that of **IIe** by 5.1 kcal/mol, and the overall stabilization energy is larger by 10 kcal/mol, again favoring **Ie** over **IIe**.

Our results, taken together, seem to indicate that 2-alkoxy-5(4*H*)-oxazolones (**I**) do not possess an inherently higher chiral stability than 2-alkyl-5(4*H*)-oxazolones (**II**); rather, they are more reactive toward the addition of amine-type nucleophiles. Thus, the outcome (in terms of the enantiomeric purity of the product) of a peptide-bond forming reaction, where a 2-alkoxy-5(4*H*)-oxazolone is involved, is the result of a competition between the relative rates of oxazolone consumption by the amine nucleophile and of oxazolone racemization. In most instances such balance can be expected to be favorable enough, owing to the higher reactivity of 2-alkoxy-5(4*H*)-oxazolones compared to their 2-alkyl counterparts. However, any factor which could either slow down peptide bond formation (*e.g.*, steric hindrance) or enhance oxazolone racemization (*e.g.*, nature of the substituent at position 4, presence of excess base) should be carefully scrutinized.

Supporting Information Available: Tables giving crystal data, atomic coordinates, isotropic and anisotropic displacement parameters, bond lengths and angles, hydrogen coordinates, and torsion angles and figures showing atom numbering for **Ia** and **Ib** (17 pages). See any current masthead page for ordering and Internet access instructions.

JA9637863

(36) Benoiton, N. L.; Chen, F. M. F. In *Peptides. Structure and Function*; Rivier, J. E., Marshall, G. R., Eds.; ESCOM: Leiden, 1990; pp 889−891.
(37) Benoiton, N. L.; Lee, Y. C.; Chen, F. M. F. *Int. J. Pept. Protein Res.* **1993**, *41*, 587−594.